

1           **Fe pre-enrichment: a new method to counteract iron loss**  
2                           **in experiments on basaltic melts**

3                                   **Revision 2**

4           **YANN-AURELIEN BRUGIER, MARINA ALLETTI, AND MICHEL PICHAVANT**

5  
6           Institut des Sciences de la Terre d'Orléans (ISTO), UMR 7327, Université d'Orléans, 45071  
7           Orléans, France and ISTO, UMR 7327, CNRS, 45071 Orléans, France and ISTO, UMR 7327,  
8                                   BRGM, BP 36009 Orléans, France

9  
10                                   **ABSTRACT**

11           Capsule pre-saturation has been traditionally employed to circumvent Fe loss from the  
12           charge to the container in petrological experiments. However, the method is time-consuming  
13           and fraught with theoretical and practical difficulties. An alternative method, based on the use  
14           of starting materials pre-enriched in Fe, is presented. Test experiments on two natural basalts,  
15           both non Fe-enriched and Fe-enriched with the addition of Fe oxides, have been carried out at  
16           1 atm and 50 MPa (H<sub>2</sub>O-saturated), 1200 and 1250°C, between NNO and NNO-1 and in Pt  
17           and Au<sub>80</sub>Pd<sub>20</sub> capsules. Glasses and capsules were analyzed by electron microprobe. Fe-  
18           concentrations in the capsule near the glass interface strongly depend on the capsule material,  
19           being 5-10 times less for Au<sub>80</sub>Pd<sub>20</sub> than for Pt. For non Fe-enriched compositions, Fe loss  
20           reaches -15% (Au<sub>80</sub>Pd<sub>20</sub>) and -60% (Pt). Increasing the level of Fe-enrichment reduces Fe  
21           loss, the amount of Fe alloyed with the capsule being compensated by the amount of Fe added  
22           to the starting composition. FeO<sub>t</sub> concentrations in high pressure glasses bracket the nominal  
23           FeO<sub>t</sub> of the two starting basalts, demonstrating that Fe alloying has been successfully  
24           counteracted. Combination of AuPd containers with Fe pre-enriched starting materials offers

25 excellent perspectives to solve the Fe loss issue in high pressure experiments on basaltic  
26 compositions.

27 **Keywords:** experiments, capsules, iron loss, pre-enrichment, basalts

28

29

## INTRODUCTION

30 Fe loss from the charge to the container is one of the most difficult problems in  
31 experimental petrology. Classically, in a high pressure experiment, the charge is contained in  
32 a chemically inert noble metal such as Pt, Au, or Ag (e.g., Chou 1986). For temperatures <  
33 1050°C, Au capsules are commonly used. However, the relatively low melting point of Au  
34 makes it inappropriate for experiments on basaltic systems. The use of Pt enables working at  
35 temperatures > 1050°C but Pt is known to interact strongly with the charge, leading to the  
36 formation of a PtFe alloy, which removes most of the Fe from the starting material (Stern and  
37 Wyllie 1975). Various methods have been proposed to mitigate Fe loss, the most commonly  
38 used being capsule Fe *pre-saturation* (see Grove 1982). This method involves the preparation  
39 at 1 atm of an alloy (PtFe in early studies) in equilibrium with the Fe-bearing charge at high  
40 temperature and pressure, and the use of that alloy as a container, instead of pure Pt (e.g.,  
41 Ford 1978; Grove 1982). More recently, AuPd alloys have attracted much interest as a  
42 substitute to Pt because of their lower susceptibility to alloying with Fe (Kawamoto and  
43 Hirose 1994). However, large amounts of Fe can dissolve in AuPd alloys depending on  $fO_2$   
44 (Hall et al. 2004; Di Carlo et al. 2006; Barr and Grove 2010; Balta et al. 2011). Therefore, the  
45 Fe pre-saturation approach has been extended to AuPd capsules (Gaetani and Grove 1998;  
46 Barr and Grove 2010; Balta et al. 2011 and references therein).

47 There are however several theoretical and practical difficulties with the Fe pre-saturation  
48 method. Balta et al. (2011) emphasized that defining the conditions needed to saturate either  
49 Pt or AuPd with the proper amount of Fe for a high pressure experiment is difficult. Even

50 after the correct 1 atm pre-saturation conditions are determined for one high pressure  
51 experiment, these conditions will differ from those needed for the next experiment in ways  
52 that are difficult to predict. In particular, one parameter that must be known precisely for the  
53 planning of the pre-saturation conditions is the  $fO_2$  of the high pressure experiment. For  
54 example, for a hydrogen buffered (i.e., constant  $fH_2$ ) gas vessel experiment with charges of  
55 different  $fH_2O$  ran together (e.g., Di Carlo et al. 2006),  $fO_2$  must vary between charges.  
56 Theoretically, for each charge, a specific alloy would need to be prepared if the pre-saturation  
57 method is to be used. Another major shortcoming of the pre-saturation method concerns the  
58 long durations necessary to prepare chemically homogeneous Fe-noble metal alloys even at  
59 high temperatures (Gaillard et al. 2003; see below). Dissolution of the Fe doping material  
60 following capsule pre-saturation can be also sluggish, the whole method being very time-  
61 consuming.

62 Difficulties with capsule Fe pre-saturation leave room for alternative approaches to reduce  
63 Fe loss in petrological experiments. In this paper, we present a new empirical method to  
64 mitigate Fe loss in high pressure experiments on basaltic systems. The method is based on a  
65 new approach, i.e., the use of starting materials *pre-enriched* in Fe.

66

67

## EXPERIMENTAL AND ANALYTICAL METHODS

68 The new method was developed within the framework of two experimental projects on  
69 natural basaltic melts which required Fe loss to be minimized. In the first project, S  
70 solubilities are measured at high temperatures (1200°C) and pressures (200 MPa) under  
71 moderately reducing conditions (i.e., at  $fO_2 \leq$  the Ni-NiO buffer, NNO), using Pt capsules in  
72 order to prevent the formation of complex Pd-, S-bearing compounds (Pichavant et al, 2006).  
73 The second project is a phase equilibrium study at 50-400 MPa, 1100-1200°C and a  $fO_2 \sim$   
74 NNO-0.5 on transitional basalts from La Réunion Island (Indian Ocean), with  $Au_{80}Pd_{20}$

75 capsules used as containers (Brugier et al., in preparation). Both projects require Fe loss to be  
76 minimized. Initially, the Fe capsule pre-saturation method was attempted but difficulties of  
77 the type summarized above were encountered. Consequently, a new methodology based on  
78 specific experiments performed at 1 atm and 50 MPa was tested, in parallel with Pt and  
79 Au<sub>80</sub>Pd<sub>20</sub> capsules.

80 A basaltic pumice from Stromboli (PST-9, Pichavant et al. 2011) and a basaltic scoria  
81 erupted in 2009 from the Piton de la Fournaise (REU-04) were used as starting materials.  
82 PST-9 has been previously experimentally investigated by Di Carlo et al. (2006) and  
83 Pichavant et al. (2009). The two samples were separately crushed, ground, and then fused at 1  
84 atm, 1400°C for 4 hours in a large Pt crucible open to air to produce crystal- and volatile-free  
85 homogeneous glasses. Chips of each starting glass were mounted in epoxy and their  
86 composition checked by electron microprobe (Table 1), the rest ground and stored in an oven  
87 at 120°C. An aliquot of each glass was used to prepare Fe-enriched (or Fe pre-enriched)  
88 starting materials by physically mixing with Fe oxide, either magnetite or hematite powders  
89 (chemical reagent grade purity). Iron enrichments are reported as wt% Fe added to the glass-  
90 oxide mixture (Tables 2 & 3).

91

## 92 **1 atm experiments**

93 The PST-9 and REU-04 starting compositions (either glass or glass-Fe oxide powders)  
94 were loaded respectively in Pt and Au<sub>80</sub>Pd<sub>20</sub> tubes (diameter: 2.5 mm, length: 20-25 mm, wall  
95 thickness: 0.2 mm), previously welded at one end. Capsules were side by side and vertically  
96 held in an alumina tube which was suspended through a Pt wire in the furnace. A 1 atm  
97 vertical gas mixing furnace was used, both at 1200°C (NNO and NNO-0.5) and 1250°C  
98 (NNO-0.5). The fO<sub>2</sub> was controlled by CO-CO<sub>2</sub> gas mixtures monitored by certified  
99 electronic flowmeters (Deines et al. 1974). Temperature was read by an S-type thermocouple

100 and is accurate to within 2°C. The sample holder and thermocouple were both located in the  
101 hot spot of the furnace. The thermal gradient is less than 5°C along the length of the capsules.

102 For the PST-9 experiments, two runs of ~ 100 h were conducted at 1200 and 1250°C with  
103 three capsules corresponding to three Fe-enrichments (0, 5, and 13 wt.% Fe added). The two  
104 72 and 194 h REU-04 experiments (1200°C), which started from a non Fe-enriched  
105 composition, were in fact classical pre-saturation experiments (Table 2). Charges were  
106 quenched by electrically fusing the Pt wire, resulting in the drop of the sample holder in the  
107 cold bottom part of the furnace. Capsules were mounted in epoxy and polished parallel to  
108 their axial plane (Fig. 1), so that they could be analyzed at different positions (top, i.e., the  
109 closest to the gas atmosphere, middle, bottom, i.e., the closest to the welded end) along their  
110 length.

111

### 112 **High pressure experiments**

113 Pt (for PST-9) and Au<sub>80</sub>Pd<sub>20</sub> (REU-04) capsules were used in the high pressure  
114 experiments similarly to those at 1 atm, apart from being welded shut. About 5 mg distilled-  
115 deionized water and ~ 50 mg of either glass or glass-Fe oxide mixture were loaded so as to  
116 yield H<sub>2</sub>O-saturated conditions. Both non Fe-enriched and Fe-enriched compositions were  
117 investigated (Table 3). Two similar experiments were performed at 50 MPa, 1200°C in a  
118 rapid-quench internally heated pressure vessel operating vertically and pressurized with an  
119 Ar-H<sub>2</sub> gas mixture (Di Carlo et al. 2006). Total pressure was recorded by a transducer  
120 calibrated against a Heise Bourdon tube gauge (uncertainty ± 2.0 MPa). The double-winding  
121 molybdenum furnace allowed a near-isothermal hot-spot zone of 2-3 cm length, with a  
122 gradient of < 3°C/cm. Temperature was monitored by two S-type thermocouples with an  
123 uncertainty of ± 5°C. H<sub>2</sub> and Ar, loaded sequentially at room temperature, were used to  
124 pressurize the vessel and to control the fO<sub>2</sub>, the two experiments being performed with the

125 same initial H<sub>2</sub> pressure (3 bar). Experimental fH<sub>2</sub> (i.e., the fH<sub>2</sub> at 50 MPa, 1200°C) was  
126 measured by CoO-CoPd sensors (Taylor et al. 1992) in separate capsules. A fO<sub>2</sub> of NNO-0.8  
127 was determined for all high pressure capsules (calculations performed with K<sub>water</sub> from Robie  
128 et al. 1979, f<sub>H<sub>2</sub>O</sub>° from Burnham et al. 1969, the NNO equation from Pownceby and O'Neill  
129 1994 and the CoPd sensor calibration of Taylor et al. 1992). Run durations were in both cases  
130 ~ 40 h, longer than most experiments with hydrous basaltic melts but approaching the  
131 duration of the 1 atm series. The experiments were terminated by drop-quenching the sample  
132 holder (Di Carlo et al. 2006). Capsules were then weighed and checked for possible leaks.  
133 Only capsules that did not show any change in weight were retained and mounted in the same  
134 way as the 1 atm capsules.

135

### 136 **Electron microprobe analyses**

137 The experimental products were analyzed with a CAMECA SX FIVE electron microprobe  
138 at ISTO, Orléans. Analyses mainly were performed along traverses several hundred μm long  
139 positioned across and perpendicular to the glass-capsule interface (Fig. 1). Analytical  
140 conditions were set, for experimental glasses, at 15 kV (acceleration voltage), 6 nA (sample  
141 current), 10 s (counting time on peak) and 5 s (counting time on background). Capsules were  
142 analyzed for Fe under the same conditions except for capsules HP4, HP5, HP7 and HP8  
143 which were analyzed at 15 kV, 30 nA, 30 s and 5 s. CoPd sensor alloys were analyzed  
144 separately under higher acceleration voltage (20 kV) and a 20 nA sample current. Relative  
145 analytical errors are 1% (SiO<sub>2</sub>, MgO, CaO), 1-2% (Al<sub>2</sub>O<sub>3</sub>), 2-4% (FeO, Na<sub>2</sub>O) and 5-10%  
146 (TiO<sub>2</sub>, K<sub>2</sub>O) for glasses. For capsules, the detection limit for Fe is around 4500 ppm,  
147 corresponding to 1.5 at% Fe, except for HP4, HP5, HP7 and HP8 (detection limit around 270  
148 ppm, corresponding to 0.08 at% Fe). For sensors, the error on the alloy composition is ± 1-2  
149 at%.

150

151

## RESULTS

### 152 1-atm experiments

153 Fe concentrations in capsules at the glass interface, obtained from the analytical traverses,  
154 depend markedly on the capsule material (Table 2). At 1200°C and NNO-0.5, they range  
155 between 4 and 10 at% Fe for Pt (reaching 24 at% Fe at 1250°C), but barely exceed the limit of  
156 detection for Au<sub>80</sub>Pd<sub>20</sub> at 1200°C, NNO (0.5-1.5 at% Fe). The Fe distribution within Au<sub>80</sub>Pd<sub>20</sub>  
157 capsules could not be precisely evaluated due to low Fe capsule concentrations and the rather  
158 elevated Fe detection limit. Charges in Pt capsules define a positive correlation between the  
159 Fe interface concentration and the level of Fe-enrichment (Table 2). Capsule Fe  
160 concentrations progressively decrease toward their external rim (Fig. 1), emphasizing the lack  
161 of bulk chemical equilibrium in our experiments. An equilibrium Fe distribution between  
162 capsule and melt is only attained near the capsule-glass interface. This stresses the long  
163 durations needed to homogenize Fe concentrations in Pt capsules of “normal” thickness (0.2  
164 mm).

165 The REU-04 glasses have  $\Delta\text{FeO}_t < 5\%$  [ $\Delta\text{FeO}_t = 100 * (\text{FeO}_t \text{ glass} - \text{FeO}_t \text{ starting}$   
166  $\text{glass}) / (\text{FeO}_t \text{ starting glass})$ , see Table 4] indicating that no significant Fe loss occurred,  
167 consistent with the low Fe interface concentrations observed in Au<sub>80</sub>Pd<sub>20</sub> capsules. In  
168 comparison, the PST-9 glasses exhibited a complex behavior in Pt capsules. Although glasses  
169 along a given traverse are chemically homogeneous, a systematic vertical stratification of  
170 glass compositions inside capsules is present. As a result, the glass data have been  
171 distinguished as a function of the position of the analytical traverse in the capsule (either top,  
172 middle or bottom, Table 4). For a given capsule and from bottom to top, glass FeO<sub>t</sub>, MgO and  
173 CaO decrease, and SiO<sub>2</sub>, Al<sub>2</sub>O<sub>3</sub>, Na<sub>2</sub>O and K<sub>2</sub>O increase. The same type of trends were  
174 observed both in non Fe-enriched and Fe-enriched charges. This compositional stratification

175 makes difficult to evaluate the pre-enrichment method. For example, for a given capsule,  
176 large differences in Fe loss ( $\Delta\text{FeO}_t$ ) occur between bottom and top glasses (e.g., -2% and -  
177 31% respectively for bottom and top in experiment 2, 5 wt% added Fe, Table 4). We attribute  
178 the observed zonations mainly to the persistence of a redox gradient inside capsules, the  
179 bottom part of the melt layer keeping oxidizing conditions (since the starting glasses were  
180 synthesized in air), only the top part of the melt layer being equilibrated with the  $f\text{O}_2$  of the  
181 gas mixture.

182

### 183 **High pressure experiments**

184 Fe-concentrations in the capsules near the glass interface range between 24 and 38 at%  
185 Fe for Pt and 3 and 4 at% Fe for  $\text{Au}_{80}\text{Pd}_{20}$  capsules (Fig. 2), higher than in the corresponding 1  
186 atm charges and in general positively correlated with the Fe-enrichment (Table 3). Both Pt  
187 and  $\text{Au}_{80}\text{Pd}_{20}$  capsules display heterogeneous Fe distributions, with Fe concentrations  
188 progressively decreasing from the glass interface toward the capsule external rim. For  
189 capsules analyzed under specific analytical conditions, the data show that Fe concentrations >  
190 1.5 at% extend to distances longer in  $\text{Au}_{80}\text{Pd}_{20}$  than in Pt (Fig. 2). Contrasting with the 1 atm  
191 glasses, the high pressure glasses are chemically homogeneous at the scale of the entire  
192 charge. For the non-enriched starting compositions,  $\Delta\text{FeO}_t$  values are elevated. They differ  
193 with the capsule material, reaching -60% (Pt) and -15% ( $\text{Au}_{80}\text{Pd}_{20}$ , Table 5). Upon increasing  
194 the level of Fe-enrichment,  $\Delta\text{FeO}_t$  progressively evolves from negative (Fe loss) to positive  
195 (Fe gain). For PST-9 in Pt capsules,  $\Delta\text{FeO}_t$  from -60%, -1%, +10%, +106% to +138% are  
196 obtained and, for REU-04 in  $\text{Au}_{80}\text{Pd}_{20}$  capsules, of -15%, -6% and +12% (Table 5). Results of  
197 representative glass traverses obtained on the two starting compositions with different Fe-  
198 enrichments are illustrated on Fig. 3. For both compositions and types of capsule materials,  
199 the nominal  $\text{FeO}_t$  of the starting basalt is bracketed by the glass  $\text{FeO}_t$  concentrations,



200 demonstrating that Fe loss toward the capsule has been effectively counteracted. The 5 wt%  
201 Fe added PST-9 composition (HP2, Table 5) illustrates the case of an optimum level of Fe  
202 pre-enrichment, defined as the amount of Fe added that yields < 5% Fe loss/gain.

203

204

## DISCUSSION

205 Our tests establish the potential of the pre-enrichment method to circumvent the Fe loss  
206 problem in experiments with basaltic melts. Working with starting materials enriched in Fe  
207 enables the influence of Fe alloying with the capsule material to be counteracted. The method  
208 has been successfully tested on both Pt and Au<sub>80</sub>Pd<sub>20</sub> capsules, at a pressure of 50 MPa,  
209 relatively high temperatures (1200°C) and moderately reducing fO<sub>2</sub> (from NNO to NNO-1).  
210 Under more reducing conditions, more Fe would alloy with capsule materials but the method  
211 should still be applicable in principle. It is important to stress that the proposed pre-  
212 enrichment method is empirical and should be adjusted for each particular set of starting  
213 compositions and experimental conditions. In particular, the experimental duration should be  
214 considered as a variable since equilibrium between melt and capsule is not attained in  
215 experiments of a few days on basaltic melts and, therefore, Fe loss is expected to increase  
216 with experimental duration, all other parameters being equal.

217 In our experiments, the additional Fe was introduced as Fe oxide. This has the advantage  
218 of simplicity and flexibility, since Fe enrichments can be sensitively adjusted. Results show  
219 that changing the type of Fe oxide (magnetite vs. hematite) does not influence the final glass  
220 compositions. Fe oxides rapidly dissolve in basaltic melts under our experimental conditions.  
221 The vertical stratification of glass compositions in the 1 atm Pt charges is not the result of Fe  
222 oxide sedimentation. In contrast with the 1 atm charges, the high pressure glass layers are  
223 chemically homogeneous indicating that Fe diffuses rapidly in the melt. However, our tests  
224 were conducted at high temperatures, above the liquidus and for hydrous melts. Other

225 procedures might be needed if the pre-enrichment method is to be used at lower temperatures  
226 (or under H<sub>2</sub>O-poor conditions), because (1) Fe oxide dissolution might take more time and  
227 (2) Fe might diffuse less rapidly in the melt. It is important to recognize that the success of the  
228 approach is based on a marked diffusivity contrast between Fe in capsule (slow) and Fe (bulk)  
229 in the melt (fast). Use of Fe-enriched glasses instead of glass-Fe oxide mixtures would  
230 eliminate the oxide dissolution step. However, we caution that the method needs further  
231 testing under conditions leading to slow bulk melt Fe diffusivities.

232 In addition to the pre-enrichment methodology, several aspects of this study are worth  
233 being emphasized. *First*, our results confirm the quite good performance of Au<sub>80</sub>Pd<sub>20</sub> capsule  
234 materials with respect to alloying with Fe. At 1200°C, Fe concentrations (at the glass-capsule  
235 interface) are 0.5-1.5 at% Fe in the 1 atm NNO experiments, increasing to 2-4 at% Fe in the  
236 high pressure NNO-0.8 experiments. These Fe concentrations are consistent with the  
237 measurements of Balta et al. (2011), noticing that their Au<sub>74</sub>Pd<sub>26</sub> alloys were equilibrated with  
238 pure Fe oxide and with their calculations for equilibration with a Kilauea basalt. We stress  
239 that, for experiments on basaltic melts at around NNO, Fe interface concentrations for AuPd  
240 alloys are 5-10 times less than for Pt. Yet, these concentrations are sufficient to affect the  
241 FeO<sub>i</sub> concentration of the encapsulated melt. In addition to differences in interface  
242 concentrations between capsule materials, Fe diffuses to longer distances in Au<sub>80</sub>Pd<sub>20</sub> than in  
243 Pt capsules. In our high pressure experiments at NNO-0.8, Fe losses with Au<sub>80</sub>Pd<sub>20</sub> capsules  
244 are -15% (Table 5). Comparable Fe losses (-13% on average) were reported by Di Carlo et al.  
245 (2006) despite fO<sub>2</sub> (between NNO-0.1 and NNO+2.3) being on average higher than in this  
246 study. Although these Fe losses are significant, the use of Au<sub>80</sub>Pd<sub>20</sub> instead of Pt (Fe loss of -  
247 60%, HP1, Table 5) clearly represents a major improvement. We conclude that the  
248 combination of AuPd containers and Fe pre-enriched starting materials offers excellent  
249 perspectives to solve the Fe loss issue in high pressure experiments on basaltic compositions,

250 when sulfur is not involved. Indeed, Au-Pd alloys tend to react with S to form complex Pd-  
251 and S-bearing compounds (Pichavant et al, 2006), weakening the capsule walls and falsifying  
252 the composition of the resulting glasses. *Second*, the melt zonation problem encountered  
253 provides an additional illustration of the difficulty to apply 1 atm methodologies to high  
254 pressure experiments. In our 1 atm experiments, chemical stratification of the melt prevented  
255 precise evaluation of Fe gains/losses and so our tests remain inconclusive. Furthermore,  
256 chemical gradients in the melt affected all major oxides in addition to FeO<sub>t</sub>, thus introducing a  
257 bias on melt composition that is not limited to Fe. More work is needed if the pre-enrichment  
258 method is to be applied to 1 atm experiments. *Third*, compared to the traditional capsule pre-  
259 saturation, the pre-enrichment method presents important advantages. Capsule preparation at  
260 1 atm prior to the high pressure experiment (synthesis of alloy, removal of Fe doping material,  
261 cleaning) is totally avoided, which saves time. Fe incorporation to the capsule takes place *in*  
262 *situ* during the high pressure experiment and, so, no estimation of the alloy composition under  
263 high pressure conditions (e.g., Barr and Grove 2010) is needed. Overall, the proposed method  
264 is fast, easy to implement, and robust even if the optimum level of Fe pre-enrichment is left to  
265 be empirically determined.

266

267

## IMPLICATIONS

268 We have presented a new methodology to counteract Fe loss from experimental charges  
269 to capsule materials in high temperature/high pressure experimental studies. The method is  
270 based on the use of starting materials pre-enriched in Fe. During the experiment, Fe alloys  
271 with the capsule material but the amount of Fe lost to the capsule is compensated by the  
272 amount of Fe added to the starting composition. Fe pre-enrichment has been demonstrated to  
273 work at high pressure (50 MPa), high temperature (1200°C), moderately reducing fO<sub>2</sub> (NNO-  
274 0.8) and for both Pt and Au<sub>80</sub>Pd<sub>20</sub> capsule materials. The method is empirical, i.e., an optimum

275 level of Fe enrichment must be determined for each particular set of starting compositions and  
276 experimental conditions, the latter including the run duration. Although tested on hydrous  
277 basaltic melts, the method offers potential for other types of experimental conditions and  
278 compositions, and is highly adaptable. Compared to the traditional pre-saturation, Fe pre-  
279 enrichment eliminates the need to prepare appropriate container capsules at 1 atm prior to  
280 high pressure experiments; estimating the alloy composition in the high pressure experiment  
281 becomes unnecessary. For high pressure experiments on basaltic compositions under  
282 moderately reducing  $fO_2$  such as volatiles solubility and phase equilibria, the combination of  
283 AuPd containers and Fe pre-enriched starting materials provides excellent perspectives to  
284 solve the Fe loss problem.

285

286

#### ACKNOWLEDGEMENTS

287 This work was supported by the VUELCO (FP7 EC) and DEGAZMAG (ANR) projects.  
288 Ida Di Carlo is acknowledged for her contribution to the electron microprobe analyses. We  
289 thank Brian Balta, Etienne Médard and Thomas Shea for their helpful reviews.

290

291

#### REFERENCES CITED

- 292 Balta, J.B., Beckett, J.R., and Asimow, P.D. (2011) Thermodynamic properties of alloys of gold-74/palladium-  
293 26 with variable amounts of iron and the use of Au-Pd-Fe alloys as containers for experimental petrology.  
294 American Mineralogist, 96, 1467-1474.
- 295 Barr, J. and Grove, T.L. (2010) AuPdFe ternary solution model and applications to understanding the  $fO_2$  of  
296 hydrous, high-pressure experiments. Contributions to Mineralogy and Petrology, 160, 631-643.
- 297 Burnham, C.W., Holloway, J.R., and Davis, N.F. (1969) Thermodynamic properties of water to 1000°C and  
298 10000 bars. The Geological Society of America Special Paper 132, 96 p.
- 299 Chou, I.-M. (1986) Permeability of precious metals to hydrogen at 2 kb total pressure and elevated temperatures.  
300 American Journal of Science, 286, 638-658.

- 301 Deines, P., Nafziger, R.H., Ulmer, G.C., and Woermann, E. (1974) Temperature-oxygen fugacity tables for  
302 selected gas mixtures in the system C-H-O at one atmosphere total pressure. Bulletin of the Earth and  
303 Mineral Sciences Experiment Station, Number 88, Pennsylvania State University.
- 304 Di Carlo, I., Pichavant, M., Rotolo, S. G., and Scaillet, B. (2006) Experimental crystallization of a high-K arc  
305 basalt: the golden pumice, Stromboli volcano (Italy). *Journal of Petrology* 47, 1317-1343.
- 306 Ford, C.E. (1978) Platinum-iron alloy sample containers for melting experiments on iron-bearing rocks.  
307 *Mineralogical Magazine*, 42, 271-275.
- 308 Gaetani, G.A. and Grove, T.L. (1998) The influence of water on melting of mantle peridotite. *Contributions to*  
309 *Mineralogy and Petrology*, 131, 323-346.
- 310 Gaillard, F., Pichavant, M., and Scaillet, B. (2003) Experimental determination of activities of FeO and Fe<sub>2</sub>O<sub>3</sub>  
311 components in hydrous silicic melts under oxidizing conditions. *Geochimica et Cosmochimica Acta*, 67,  
312 4389-4409.
- 313 Grove, T.L. (1982) Use of FePt alloys to eliminate the iron loss problem in 1 atmosphere gas mixing  
314 experiments: theoretical and practical considerations. *Contributions to Mineralogy and Petrology*, 78, 298-  
315 304.
- 316 Hall, L.J., Brodie, J., Wood, B.J., and Carroll, M.R. (2004) Iron and water losses from hydrous basalts contained  
317 in Au<sub>80</sub>Pd<sub>20</sub> capsules at high pressure and temperature. *Mineralogical Magazine*, 68, 75-81.
- 318 Kawamoto, T. and Hirose, K. (1994) Au-Pd sample containers for melting experiments on iron and water-  
319 bearing systems. *European Journal of Mineralogy* 6, 381-385.
- 320 Pichavant, M., Scaillet, B., Di Carlo, I., Rotolo, S., Métrich, N. (2006) Sulfur in hydrous, oxidized basaltic  
321 magmas: phase equilibria and melt solubilities. *Eos Trans. AGU*, 87 (36), Jt. Assem. Suppl., Abstract V41C-  
322 02
- 323 Pichavant, M., Di Carlo, I., Le Gac, Y., Rotolo, S., and Scaillet, B. (2009) Experimental constraints on the deep  
324 magma feeding system at Stromboli volcano, Italy. *Journal of Petrology* 50, 601-624.
- 325 Pichavant, M., Pompilio, M., D'Orlando, C., and Di Carlo, I. (2011) Petrography, mineralogy and geochemistry  
326 of a primitive pumice from Stromboli: implications for the deep feeding system. *European Journal of*  
327 *Mineralogy* 23, 499-517.
- 328 Pownceby, M. I. and O'Neill, H. St. C. (1994) Thermodynamic data from redox reactions at high temperatures.  
329 III. Activity-composition relations in Ni-Pd alloys from EMF measurements at 850-1250 K and calibration  
330 of the NiO + Ni-Pd assemblage as a redox sensor. *Contributions to Mineralogy and Petrology* 116, 327-339.

- 331 Robie, R. A., Hemingway, B. S., and Fisher, J. R. (1979) Thermodynamic properties of minerals and related  
332 substances at 298.15 K and 1 bar ( $10^5$  pascals) pressure and at higher temperatures. US Geological Survey  
333 Bulletin 1452.
- 334 Stern, C.R. and Wyllie, P.J. (1975) Effect of iron absorption by noble-metal capsules on phase boundaries in  
335 rock-melting systems. American Mineralogist, 60, 681-689.
- 336 Taylor, J. R., Wall, V. J., and Pownceby, M. I. (1992) The calibration and application of accurate redox sensors.  
337 American Mineralogist, 77, 284-295.

338

339

### FIGURE CAPTIONS

340 **Fig. 1.** Distribution of Fe (Fe K $\alpha$  intensity map, 15 kV acceleration voltage) in 1 atm charge 5  
341 (experimental conditions in Table 2) illustrating the chemically homogeneous glass layer and  
342 the progressive decrease in Fe concentration in the Pt capsule from the glass interface toward  
343 its external rim.

344

345 **Fig. 2.** Representative electron microprobe traverses through different capsules from the same  
346 high pressure experiment. Fe concentrations in capsules (at%) are plotted against distance  
347 ( $\mu\text{m}$ ). Experimental conditions in Table 3. (a) Pt capsule, charge HP5. Error bars are smaller  
348 than symbols. (b) Au<sub>80</sub>Pd<sub>20</sub> capsule, charge HP4. Melt compositions and Fe enrichments in  
349 Table 5. Note the heterogeneity in the Fe distribution inside capsules, especially in (a), the  
350 difference in Fe interface concentrations between Pt and Au<sub>80</sub>Pd<sub>20</sub> and the longer Fe diffusion  
351 distances in Au<sub>80</sub>Pd<sub>20</sub> than in Pt.

352

353 **Fig. 3.** Results of electron microprobe traverses showing glass FeO<sub>t</sub> concentrations (wt%,  
354 normalized to 100%) plotted against distance ( $\mu\text{m}$ ) for the high pressure charges.  
355 Experimental conditions in Table 3. Glass averages in Table 5. Data points are distinguished  
356 with Fe pre-enrichments expressed as wt% Fe added to the glass. (a) PST-9 charges ran in Pt  
357 capsules. (b) REU-04 charges ran in Au<sub>80</sub>Pd<sub>20</sub> capsules. The horizontal lines mark the FeO<sub>t</sub> of

358 the starting PST-9 and REU-04 glasses (Table 1). In (a), the starting PST-9 glass composition  
359 is bracketed by charges HP2 and HP5 (both with 5% Fe added) and, in (b), the REU-04 by  
360 charges HP8 (2 wt% Fe) and HP4 (10 wt% Fe).

361

362

**Table 1.** Composition of starting glasses.

Oxide	PST-9	REU-04
SiO <sub>2</sub>	50.6	50.5
TiO <sub>2</sub>	0.88	2.56
Al <sub>2</sub> O <sub>3</sub>	16.2	13.8
FeO <sub>t</sub>	7.95	10.6
MnO	0.13	0.14
MgO	7.16	7.63
CaO	12.1	11.3
Na <sub>2</sub> O	2.38	2.64
K <sub>2</sub> O	1.88	0.69
P <sub>2</sub> O <sub>5</sub>	0.61	0.17
Cr <sub>2</sub> O <sub>3</sub>	0.03	0.05
NiO	0.05	0.03
Total	99.7	99.1

Data are averages calculated on multiple (10-50) glass analyses. Concentrations are normalized to 100%; total is unnormalized.



**Table 2.** Experimental conditions for 1 atmosphere experiments.

Charge#	1	2	3	4	5	6	7	8
T (°C)	1200	1200	1200	1250	1250	1250	1200	1200
Log fO <sub>2</sub>	- 8.2	- 8.2	- 8.2	- 8.2	- 8.2	- 8.2	- 7.7	- 7.7
ΔNNO <sup>1</sup>	- 0.5	- 0.5	- 0.5	- 0.5	- 0.5	- 0.5	0	0
Capsule material	Pt	Pt	Pt	Pt	Pt	Pt	Au <sub>80</sub> Pd <sub>20</sub>	Au <sub>80</sub> Pd <sub>20</sub>
Wt% Fe added <sup>2</sup>	0	5	13	0	5	13	0	0
Duration (h)	110	110	110	100	100	100	72	194
Fe in capsule (% at.) <sup>3</sup>	4	5-8	7-10	4-7	8-11	20-24	0.5	1.5
Glass	PST-9	PST-9	PST-9	PST-9	PST-9	PST-9	REU-04	REU-04

<sup>1</sup>Log fO<sub>2</sub> charge – Log fO<sub>2</sub> NNO at the same P and T. NNO equation from Pownceby and O'Neill (1994).

<sup>2</sup>Amount of Fe (metallic iron) added to the glass in wt%.

<sup>3</sup>Fe concentration in capsule at the glass interface.

**Table 3.** Experimental conditions for high pressure experiments.

Experiment	1200°C, 485 bar, 42 h				1200°C, 475 bar, 40h			
	HP1	HP2	HP3	HP4	HP5	HP6	HP7	HP8
Log fO <sub>2</sub>	-8.5	-8.5	-8.5	-8.5	-8.5	-8.5	-8.5	-8.5
ΔNNO <sup>1</sup>	-0.8	-0.8	-0.8	-0.8	-0.8	-0.8	-0.8	-0.8
Capsule material	Pt	Pt	Pt	Au <sub>80</sub> Pd <sub>20</sub>	Pt	Pt	Au <sub>80</sub> Pd <sub>20</sub>	Au <sub>80</sub> Pd <sub>20</sub>
Wt% Fe added <sup>2</sup>	0	5	13	10	5	13	0	2
Fe in capsule (% at.) <sup>3</sup>	24-25	26-27	30-33	3.2-3.4	26	38	4	2.9
Glass	PST-9	PST-9	PST-9	REU-04	PST-9	PST-9	REU-04	REU-04

<sup>1</sup>Log fO<sub>2</sub> charge – Log fO<sub>2</sub> NNO at the same P and T. NNO equation from Pownceby and O'Neill (1994).

<sup>2</sup>Amount of Fe (metallic iron) added to the glass in wt%.

<sup>3</sup>Fe concentration in capsule at the glass interface.

**Table 4.** Composition of representative 1 atm experimental glasses.

Oxide	1	2	2	3	3	4	5	5	6	6	7	8
SiO <sub>2</sub>	50.2	49.9	53.8	49.3	54.3	51.1	49.3	51.7	46.2	52.4	48.8	49.7
TiO <sub>2</sub>	1.00	1.03	1.06	0.90	0.93	0.85	0.89	0.82	0.79	0.80	2.53	2.52
Al <sub>2</sub> O <sub>3</sub>	16.6	16.3	17.0	16.4	17.0	17.3	16.7	17.1	15.7	16.9	13.6	13.7
FeO <sub>t</sub>	7.54	7.79	5.48	9.86	6.30	7.24	9.95	7.89	15.2	9.95	10.8	10.6
MnO	0.20	0.16	0.13	0.17	0.12	nd	nd	nd	nd	nd	0.17	0.18
MgO	7.25	7.72	6.44	6.65	5.45	6.40	6.31	5.82	6.31	4.7	8.22	7.91
CaO	11.5	11.4	9.62	10.9	8.75	12.2	11.9	11.7	11.69	9.53	12.4	12.2
Na <sub>2</sub> O	2.77	2.60	2.88	2.73	3.12	2.57	2.56	2.55	2.14	2.80	2.53	2.26
K <sub>2</sub> O	2.30	2.40	2.77	2.34	3.23	1.94	1.89	1.97	1.52	2.47	0.65	0.55
P <sub>2</sub> O <sub>5</sub>	0.67	0.65	0.71	0.71	0.70	0.49	0.50	0.51	0.48	0.48	0.31	0.29
Cr <sub>2</sub> O <sub>3</sub>	0.04	0.04	0.05	0.05	0.04	nd	nd	nd	nd	nd	0.03	0.03
NiO	0.02	0.01	0.02	0.01	0.01	nd	nd	nd	nd	nd	0.01	0.06
Total	97.7	97.0	97.6	97.6	97.0	97.7	96.9	100	97.6	97.7	95.7	97.8
Wt% Fe added <sup>1</sup>	0	5	5	13	13	0	5	5	13	13	0	0
ΔFeO <sub>t</sub> (% relative)	-5	-2	-31	+24	-21	-9	+25	-1	+91	+25	+2	0
Position	bottom	bottom	top	bottom	top	bottom	bottom	top	bottom	top	middle	middle
Glass	PST-9	PST-9	PST-9	PST-9	PST-9	PST-9	PST-9	PST-9	PST-9	PST-09	REU-04	REU-04

Charge# as in Table 2.

Data are averages calculated on multiple (10-50) glass analyses. Concentrations are normalized to 100%; total is unnormalized.

$\Delta\text{FeO}_t = 100 * (\text{FeO}_t \text{ glass} - \text{FeO}_t \text{ starting glass}) / (\text{FeO}_t \text{ starting glass})$ .

<sup>1</sup>Amount of Fe (metallic iron) added to the glass in wt%.

**Table 5.** Composition of representative high pressure experimental glasses.

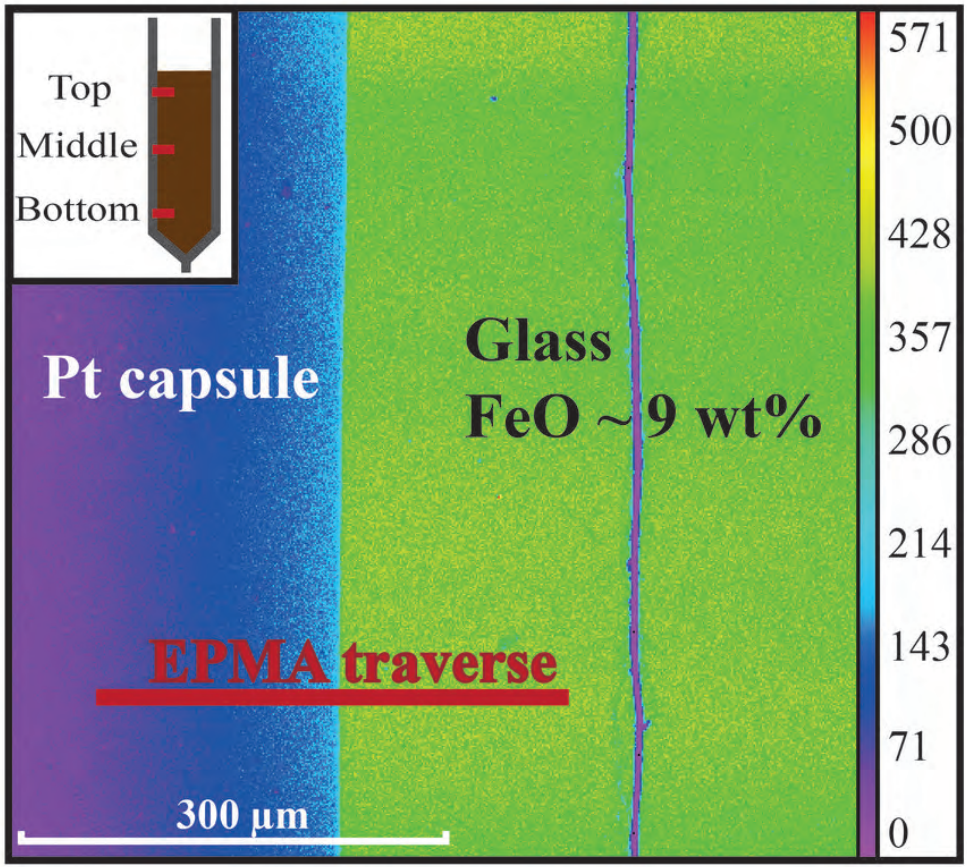
Oxide	HP1	HP2	HP3	HP4	HP5	HP6	HP7	HP8
SiO <sub>2</sub>	53.2	51.0	46.5	49.6	49.8	44.3	51.3	50.5
TiO <sub>2</sub>	0.98	0.87	0.79	2.59	0.90	0.79	2.61	2.55
Al <sub>2</sub> O <sub>3</sub>	17.3	17.2	15.0	14.2	16.9	14.8	14.0	13.7
FeO <sub>t</sub>	3.15	7.84	16.4	11.9	8.76	18.9	8.96	9.92
MnO	0.14	0.16	0.13	0.11	0.15	0.15	0.16	0.19
MgO	6.90	6.51	5.87	7.23	6.47	5.90	7.92	8.08
CaO	13.0	11.9	10.7	11.4	12.0	10.6	11.8	11.7
Na <sub>2</sub> O	2.45	2.06	2.14	1.93	2.46	2.20	2.43	2.57
K <sub>2</sub> O	2.21	2.01	1.96	0.73	2.06	1.78	0.62	0.59
P <sub>2</sub> O <sub>5</sub>	0.67	0.52	0.53	0.36	0.49	0.46	0.21	0.20
Cr <sub>2</sub> O <sub>3</sub>	0.01	0.00	0.00	0.02	0.01	0.01	0.03	0.04
NiO	0.01	0.00	0.00	0.00	0.04	0.04	0.07	0.05
Total	92.7	93.5	93.6	92.7	94.1	95.1	96.0	95.4
Wt% Fe added <sup>1</sup>	0	5	13	10	5	13	0	2
$\Delta\text{FeO}_t$ (% relative)	-60	-1	+106	+12	+10	+138	-15	-6
Position	middle	middle	middle	all	bottom	bottom	all	all
Glass	PST-9	PST-9	PST-9	REU-04	PST-9	PST-9	REU-04	REU-04

Charge# as in Table 3.

Data are averages calculated on multiple (10-50) glass analyses. Concentrations are normalized to 100%; total is unnormalized.

$\Delta\text{FeO}_t = 100 * (\text{FeO}_t \text{ glass} - \text{FeO}_t \text{ starting glass}) / (\text{FeO}_t \text{ starting glass})$ .

<sup>1</sup>Amount of Fe (metallic iron) added to the glass in wt%.



Brugier et al. Fig. 1

